Ripening Stage in Mechanical Properties of Chopin Apples for Static FEM Model Construction

Monika Słupska *, Roman Stopa , Adam Figiel

Posted Date: 1 April 2025

doi: 10.20944/preprints202409.0825.v2

Keywords: Apple tissue biomechanics; Non-destructive bruise evaluation; Finite element modeling of soft biological materials; Ripeness-dependent mechanical properties; Micro-CT in food texture analysis

 doi:10.20944/preprints202409.0825.v2

Article

Ripening Stage in Mechanical Properties of Chopin Apples for Static FEM Model Construction

Monika Słupska [1]*, Roman Stopa [1] and Adam Figiel [2]

[1] Department of Engineering Fundamentals, Institute of Agricultural Engineering, Wrocław University of Environmental and Life Sciences, Chełmońskiego 37, 51-630, Wroclaw, Poland

[2] Department of Thermal Technology and Process Engineering, Institute of Agricultural Engineering, Wroclaw University of Environmental and Life Sciences, Chełmońskiego 37, 51-630, Wroclaw, Poland

* Correspondence: monika.slupska@upwr.edu.pl; WhatsApp.: +48 785 052 155

Abstract: Most available studies on the mechanical properties of apples lack the comprehensive results needed for the construction and validation of static FEM models. Researchers typically focus on either the flesh and epidermis or the whole fruit, often overlooking the maturity stage of the examined apples. They usually report only firmness or the starch index as indicators of maturity. Furthermore, many studies use store-bought apples, which is impractical for industrial applications since this fruit has already undergone various treatments before reaching the shelf. This article aims to determine the mechanical properties of apples necessary for constructing static FEM models that are both adequate and useful for the industry. The new Polish apple variety, Chopin, was selected as the research material. The study was conducted for three stages of apple maturity: development, ripening, and senescence. Mechanical properties of the flesh and skin were determined as material data for FEM models. Force-displacement curves and pressure-force functions were examined for future model validation. Using micro-computed tomography, the bruise volumes of fruit subjected to 20%, 50%, and 80% of the destructive force were determined. Significant differences were found between apples in the senescence stage and those in the development and ripening stages. Results of Micro-Ct and the results of modified and real compression tests of whole fruit have allowed us to formulate the research hypothesis regarding the influence of flesh cracking (characterized by local drops of force), influencing the bruise visibility and detection.

Keywords: Apple tissue biomechanics; Non-destructive bruise evaluation; Finite element modeling of soft biological materials; Ripeness-dependent mechanical properties; Micro-CT in food texture analysis

1. Introduction

Creating new apple varieties is based on improving biological characteristics adapted to environment conditions, processing technologies and user requirements. The development of new varieties resistant to damages during collecting, transport and storage processes contributes to reducing losses and production demand thereby contributing to reducing financial and environmental costs [1–4]. Nevertheless, it is necessary to determine the micromechanical properties of this apple in order to compare it with other varieties.

Apples are composite materials consisting of various structural elements with different mechanical properties, but the majority of them comprise edible parenchymal tissue (flesh) [5,6]. The mechanical properties of flesh depend on the condition of cell walls and the turgor pressure of cells. From a mechanical standpoint, the fruit cell wall constitutes a robust network with a fibrous structure, providing each cell with its stable shape: a network resistant to stretching (cellulosic), a network resistant to shearing (hemicellulosic), and a network resistant to compression (pectic). Pectin is also responsible for cell adhesion strength. It is a type of polysaccharide that, in the case of apples,

 doi:10.20944/preprints202409.0825.v2

constitutes over half of the dry mass of the cell wall, thus primarily contributing to the mechanical properties of fruit. Its degradation is caused by enzymatic reactions naturally occurring in plants but can also be induced by pathogenic fungi and bacteria. Pectin enzymatic reaction affects the rheological properties, porosity, and ionic status of the cell wall. Pectins are also the main component of the middle lamella which binds adjacent cells, therefore they are considered to be the main determinant of the mechanical properties of the cell wall and plant tissue. Therefore, accurate determination of the stage of fruit ripeness and carrying out tests for different stages of fruit ripeness are so important in all fruit strength tests [7–12].

Unfortunately, most of the available studies on the mechanical properties of apples do not include all the results necessary for the construction and validation of FEM models of the apples. Scientists focus either on studying the flesh and epidermis or the whole fruit, often neglecting the maturity stage of the examined fruit. They frequently report only firmness or the starch index as indicators of the maturity stage. Moreover, research is very often conducted on store-bought apples, which is meaningless for practical applications in the industry, as at this stage, we only see the consequences of the treatments the fruit underwent before reaching the shelf [13–16].

Of course, some research is aimed at presenting new methodologies rather than creating a database of the strength properties of a specific variety. Among the methods for measuring the mechanical properties of apple fruit, various tests can be distinguished, including uniaxial tests, multiaxial tests, tests on non-uniform samples, in situ tests, dynamic tests, as well as micro- and nanomechanical tests. Each of these methods has its advantages and disadvantages, and the choice depends on the research goal and available resources. In addition to the test method itself, it is also important to establish measurement parameters such as force, deformation, strain, modulus of elasticity, Poisson's ratio, absorbed energy, acoustic response, surface pressures, and destructive stresses. The study of the mechanical properties of fruit tissues is an area of intense scientific research, crucial in assessing the quality and durability of fruit in harvesting, transportation, and storage processes. It is also worth noting that these methods are constantly being improved. In recent years, much research has focused on the use of modern technologies enabling both destructive and non-destructive analyses. These studies can also be divided into macro, micro, nano scales, and those conducted at the atomic level [7,17–23]. It opens the new field of fruit mechanical research: non-destructive Micro-CT imaging, combined with strength tests and numerical modeling forms the basis for reverse engineering research on apple fruit tissues.

Therefore, the article presents the results of mechanical and Micro-CT tests for specific and verified apple ripeness stages, constituting a set of complete data for building FE models.

2. Materials and Methods

2.1. Research Material

The Chopin variety apples, serving as the research material, were bred and harvested by the Experimental Orchards of the Warsaw University of Life Sciences in Wilanów. Harvest dates, established by the producer based on predictions for collective, consumption, and physiological ripening stages, fell on October 13th, October 26th, and November 14th, 2022, respectively. The harvest date for the development stage of ripeness was determined using the ethylene-induced method, but additionally ethylene concentration in seed chambers was also tested for the remaining stages of maturity. The ethylene content in the seed chambers (μL/L) was assessed according to a commonly used method [24], using a gas chromatograph (HP 5890, Hewlett Packard, Palo Alto, CA, USA).

To obtain representative samples for testing, apples have been selected based on diameter, height, and weight so that these parameters fall within the average values for the variety. Height and diameter were measured using the DC-1 caliper (Ovibell GmbH & Co. KG, Mulheim, Germany) with a measurement accuracy of 0.01 mm, while weight was measured using the laboratory scale WTC

 doi:10.20944/preprints202409.0825.v2

600 (RADWAG, Psary, Poland) with a measurement accuracy of 0.001 g. The apples were tested within 24 hours after harvest.

2.2. Determination of Basic Physicochemical Properties of Fruit

In order to confirm the ripening stages, and determine the well know parameters for the apple characterization, a measurement of firmness (F), soluble solids content (SSC), and starch index (SI) were conducted to calculate the Streif Index (IS) based on these three parameters. Firmness was measured using a manual penetrometer (Facchini FT 327, Alfonsine, Italy) equipped with a cylindrical penetrating attachment with a diameter of 11.1 mm. Prior to firmness testing, the apple skin was removed. Soluble solids content was determined using a manual refractometer (RMR 200, Hanna Instruments, Woonsocket, Rhode Island, USA) [25]. Starch index (SI) was determined by immersing apple slices in an iodine solution for one minute, followed by drying and comparison with standards [26].

The Streif index (IS) was calculated using Equation (1):

$$IS = \frac{F}{SSC \cdot SI} \quad (1)$$

Where: F – firmness [kG], SSC – Soluble sugar content [%], SI – starch index [-].

Water content was determined using a gravimetric method. Freeze-drying was performed using a Labconco 4.5L lyophilizer (Kansas City, MO, USA) under the following parameters: pressure 50 Pa, collector temperature -48ºC, drying time 24 hours.

Pectins were precipitated from the solution of the tested sample using 100% acetone. Results were obtained using gravimetric methods: filtration, drying, and weighing the resulting precipitate [27].

Malic acid content was determined based on acidimetric analysis - 5 ml of juice and 100 ml of distilled water were titrated with 0.1 N NaOH to pH 8.1 (neutralization of the solution) [3].

To determine the density of the apple peel, core, and flesh, the mass-to-volume ratio method was used. The apple was carefully separated into three components: peel, core, and flesh. Each component was cut into small, measurable pieces. The mass of each component was measured using an analytical balance with an accuracy of 0.01 g. The volume was measured using the water displacement method by submerging each sample in a graduated cylinder and recording the increase in water level. Finally, the density was calculated as the ratio of mass to volume. The process was repeated for multiple samples to ensure accuracy.

2.3. Determination of Strength Properties of Apple Flesh and Skin

2.3.1. Flesh

The strength properties of flesh, for the studied stages of maturity, were determined in a compression test. For this purpose, cuboid samples of flesh were tested. Their height was no more than 1.5 times the base edge to avoid the lack of a uniaxial stress state, thus meeting the assumptions of Saint-Venant's principle. The samples were loaded using an Instron 5566 strength testing machine (Instron, Norwood, Massachusetts, USA) under quasi-static conditions at a loading speed of 1 mm·min-1. The accuracy class of the force measuring head was 0.5 according to ISO 7500-1. Figure 1b presents the average results of the conversion of force-displacement plots to a stress-strain plot, for all ripening stages of apples. The Young's Modulus values were calculated as the ratio of yield stress to strain results. Poisson's ratio values were determined based on the ratio of transverse strain to axial strain, averaged for each sample. During the tests, Poisson's ratio was also determined by measuring the strain in two mutually perpendicular directions of the sample in a compression test (Figure 1a). For this purpose, a ME45 optical extensometer (Messphysik, ZwickRoell Testing Systems, Fürstenfeld, Austria) was used and the standard equation for determining the Poisson's ratio (Equation (2)).

$$\upsilon = \varepsilon_1 \cdot \varepsilon_2^{-1} \quad (2)$$

Where: υ – Poisson's ratio [-], ε_1 - transverse strain [-], ε_2 - axial strain [-].

 doi:10.20944/preprints202409.0825.v2

This value was calculated, for each sample, throughout the entire loading range until the yield point was reached. Then the collected values were averaged for all loading ranges of each sample. The tests were carried out in 10 repetitions.

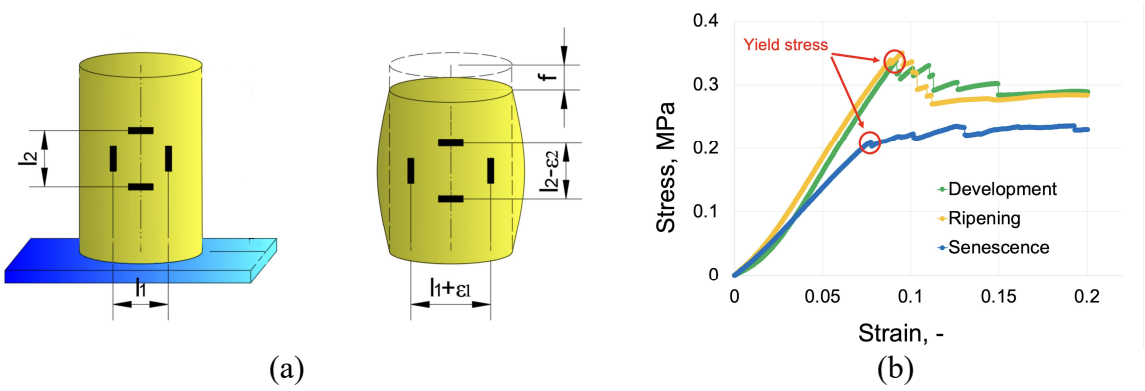

Figure 1. The method of apple flesh strength testing: (**a**) determination of Poisson's ratio method, (**b**) - determination of Elastic Modulus method.

2.3.2. Skin

The strength properties of the epidermis were determined in a tensile test. The sample preparation method is shown in Figure 2c. Similarly, to the compression test of the flesh, the samples were loaded using the strength testing machine under quasi-static conditions at a loading speed of 1 mm·min^{-1}. The Young's Modulus values were calculated based on the stress-strain curves (Figure 2b). Figure 2a presents an example of force-displacement plot used to calculate the above-mentioned stress-strain relationship. The tests were carried out in 10 repetitions.

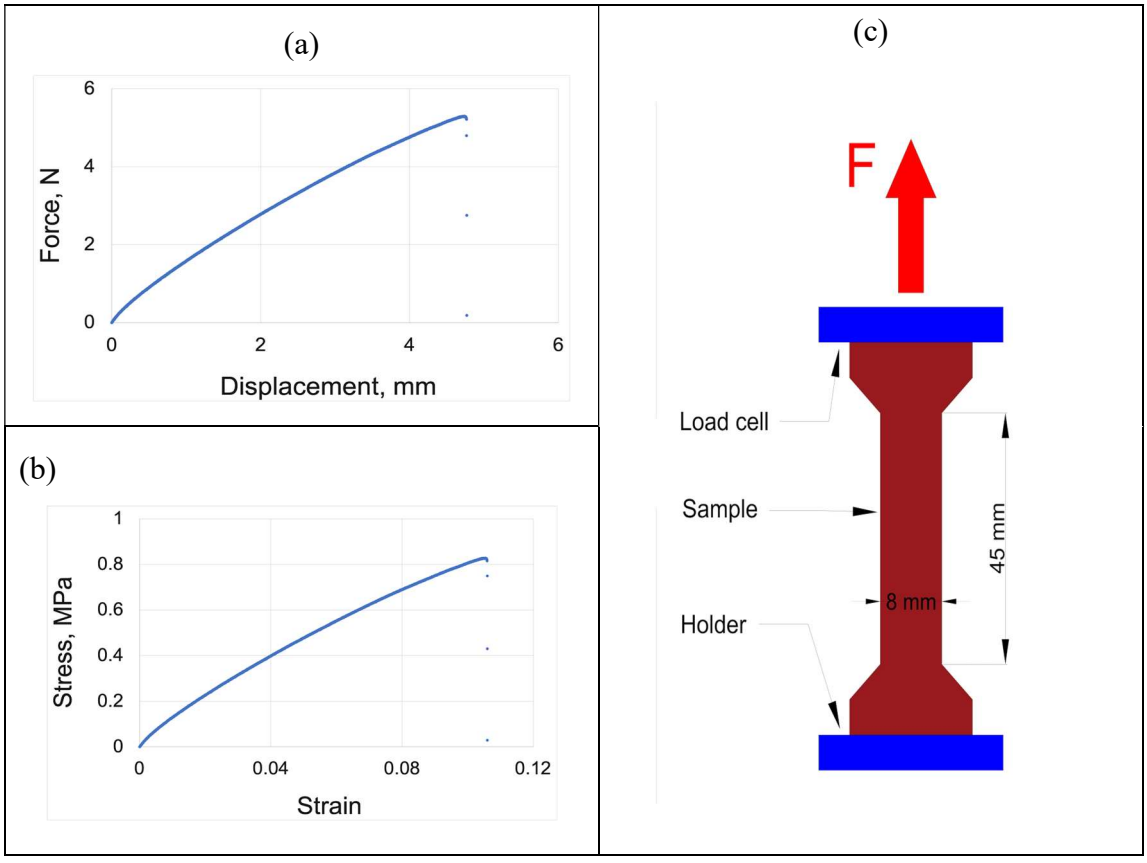

 doi:10.20944/preprints202409.0825.v2

Figure 2. The method of apple skin strength testing: (**a**) Sample graph of force as a function of displacement used to calculate stress-strain relationship, (**b**) - Sample graph of stress-strain used to calculate the Young's Modulus values, (**c**) - Tensile test scheme.

2.4. Determination of Strength Properties of Apple Fruit

The load process was measured as a function of displacement using a strength testing machine, under quasi-static conditions at a loading speed of 1 mm·min^{-1}. In addition, the distribution of the surface pressure exerted by the sample in the compression test was measured with the Tekscan I-Scan VHS System (Tekscan, Boston, Massachusetts, U.S.A). The tests were carried out in 5 repetitions.

The process of flesh cracking characteristic of fresh apple fruit (characterized by local drops in force) prevented the interpretation of the elastic properties of whole fruit. Therefore, the test data (marked in blue) were modified by compensating for these local drops (marked in red) as shown on Figure 3. This procedure required identifying the maximum force before the drop and then removing the forces leading to the sample's re-strengthening and continuing the graph with the force increasing further. Consequently, the displacement does not correspond to the actual values occurring during the test. The graph was used to visualize elastic behaviors and to demonstrate the critical points of the apple compression process.

The test modification produced graphs suited for elastic material (marked in orange), enabling the compression process to be divided into three phases: Region 1: characterized by a rapid increase in force, indicating that the apple remains flexible; Region 2: marked by an inflection point, where the rate of force increase begins to slow as the material gradually loses its elastic properties in favor of plastic behavior; Region 3: the stage where the flesh tissue along the compression axis is fully compromised, leading to cracking as the skin's structural continuity fails.

The inflection point, flesh failure point and skin failure point were determined using MatLab software, which detected changes in the slope angle of the graph indicating a transition from elastic to plastic behavior. This graph was primarily created to validate the elastic properties of FEM models [28]. In the following article, the authors demonstrate the limitations of using only elastic properties when modeling apple fruits and highlight the advantages of elastoplastic models.

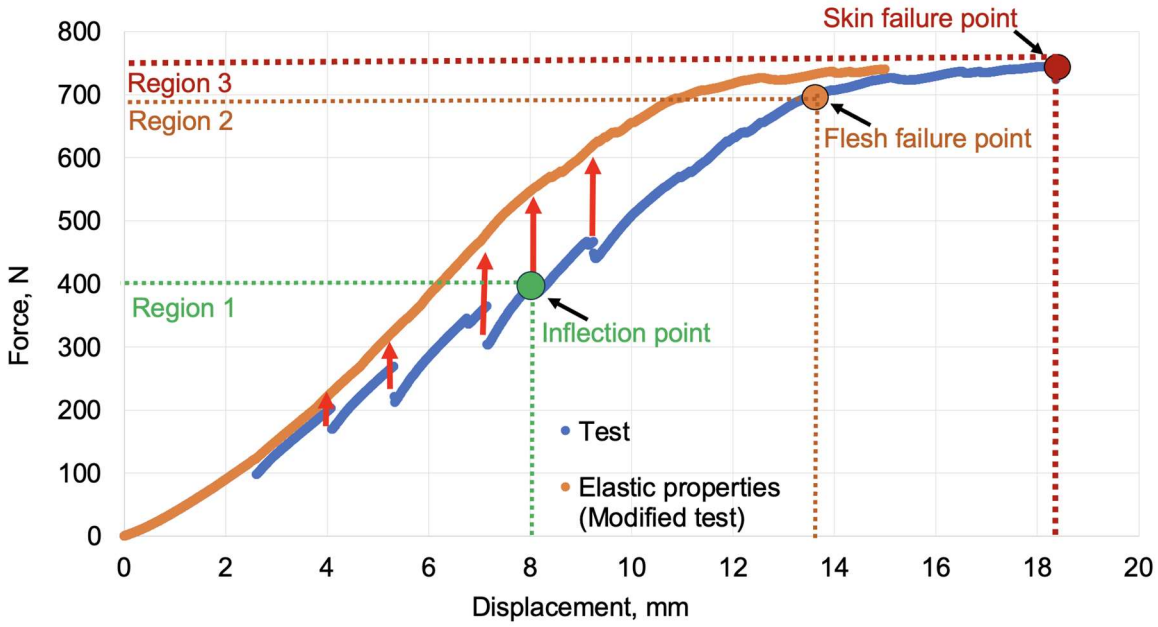

Figure 3. A method for modifying and interpreting test data.

 doi:10.20944/preprints202409.0825.v2

2.5. Determination of the Bruise Geometry and Volume Using Micro-Computed Tomography

Based on the results of apple compression tests (chapter 2.4.) at the development stage of apple maturity, the average value of the fruit failure force was determined. This value was used to determine the extent of damage to fruit at all stages of ripeness, which were subjected to loads of 20%, 50% and 80% of the average failure force. The value of the forces was 146 N, 365 N and 585 N, respectively. Immediately after loading, the fruit was scanned using a computer microtomograph Phoenix V tome x S (Waygate Technology, Hürth, Germany). Scans were performed with the following parameters: voltage 60 kV, current 350 µA, timing 333 ms, averaging every 3 frames and skipping 1 frame, sensitivity 1. As a result, a voxel resolution of 0.1 mm was achieved. The bruise geometry was measured by combining the popular bruise volume calculation method [29], with the use of VG Studio MAX software (Volume Graphics GmbH, Heidelberg, Germany), instead of using the caliper to measure bruise dimensions.

Figure 4 presents the original Micro-CT pictures from VG Studio MAX software, along with a description of the sizing of the fruit bruise geometry used to calculate the fruit bruise volume, according to the Equations (3)–(5) [30]:

$$V_1 = \frac{\pi x}{24}(3W_1 \cdot W_2 + 4x^2) \quad (3)$$

$$V_2 = \frac{\pi y}{24}(3W_1 \cdot W_2 + 4y^2) \quad (4)$$

$$V = V_1 + V_2 \quad (5)$$

Where: V_1 – volume of bruise above the contact plane [mm³], V_2 – volume of bruise below the contact plane [mm³], V – total bruise volume [mm³], W1 – width of the shorter axis of the bruise ellipse [mm], W_2 – width of the longer axis of the bruise ellipse [mm], x– bruise depth above the contact plane [mm], y – bruise depth below the contact plane [mm].

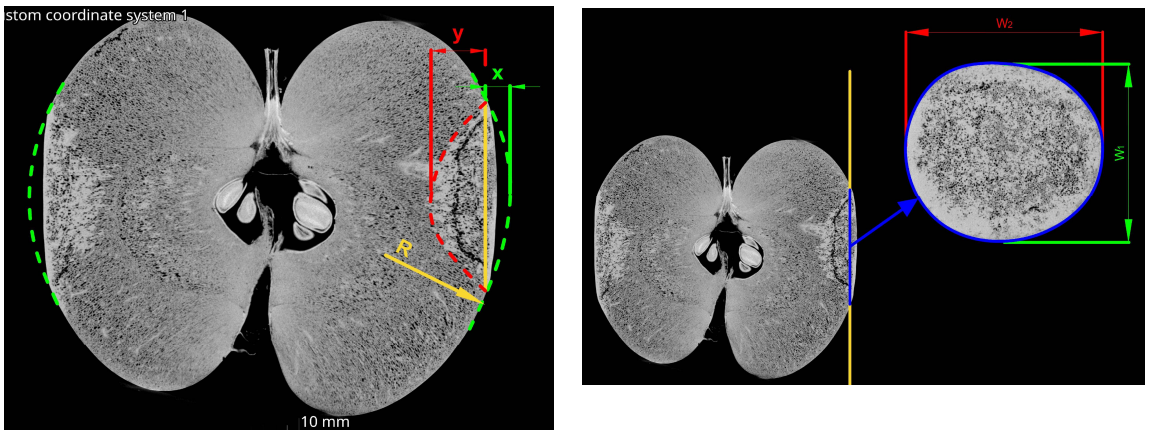

(a) (b)

Figure 4. Sizing of the fruit bruise geometry: (**a**) bruise depth, (**b**) bruise width.

3. Results

3.1. Characteristics of the Material Selected for Testing

Table 1 shows the results of testing the density, water content and geometric parameters of the fruit.

Table 1. Fruit dimensions and water content results at three ripening stages.

Stage of ripeness	Density, kg·m³	Average Diameter, mm	Average Height, mm	Water content, %

 doi:10.20944/preprints202409.0825.v2

Development	995.16±10.96	76.95±1.16	64.56±2.17	85.57±4.20
Ripening	1037.21±18.56	78.48±1.83	63.79±3.44	84.10±1.80
Senescence	1047.22±20.24	77.88±1.71	65.51±3.58	83.42±4.30

The water content in the fruit decreased with time with their physiological development, ranging from 83.42 to 85.57%. In addition, the average dimensions of fruit cores were measured. The average value of the core diameter was 32 ±2.1 mm, while the average value of the core height was 39 ±3.06 mm.

3.1. Basic Physicochemical Properties of Fruit

Table 2 presents the results of tests for firmness, SSC content, starch index and the Streif index determined on the basis of the above-mentioned parameters, as well as ethylene concentration, malic acid and pectin content at individual fruit harvest dates.

Table 2. Physicochemical characterization of the studied material for three stages of fruit ripening.

Stage of ripeness	Firmness, N	Soluble solids content, %	Starch index, -	Streif index, -	Ethylene concentration, $\mu L C_2H_4 \cdot L^{-1}$	Malic acid content, %	Pectin content, $g \cdot 100g\ s.m^{-1}$ [%]
Development	72.6 ±2.4	11.60±0.49	5±0.60	0.12	0.1	0.83	9.53
Ripening	67.7±1.6	14.00±0.25	7±0.40	0.07	12	0.78	7.20
Senescence	56.9±7.9	14.60±0.97	9±1.10	0.04	31	0.66	4.07

Based on Table 2, it can be concluded that firmness decreased from 72.6 N to 56.9 N with the stage of physiological development. The soluble solids content (SSC), as well as the starch index, increased with fruit ripeness. For ripening and senescence maturity, the values of SSC were similar and amounted to 14.00% and 14.06%, respectively, whereas in the case of senile maturity, the SSC value was significantly lower and amounted to 11.6%. The values of the Streif index were 0.12 for the stage of development maturity, 0.07 for the stage of ripening maturity and 0.04 for the stage of senescence maturity. Fruit at the senescence maturity stage exhibited the lowest malic acid content of 0.66%, whereas those at the development maturity stage had the highest content of 0.83%. For fruit at the ripening maturity stage, the value of malic acid content was 0.78%. The pectin content in fruit decreased with their maturity, reaching the values of 9.53%, 7.2% and 4.07% for development, ripening and maturity stage, respectively.

3.1. Strength Properties of Apple Flesh and Skin

Table 3 presents the results for mechanical properties of apple skin and flesh which constitute the basis for defining the material's behavior under load.

 doi:10.20944/preprints202409.0825.v2

Table 3. Results of mechanical properties of flesh and skin.

Stage of ripeness	Skin	Flesh	
	Modulus of Elasticity, MPa	Modulus of Elasticity, MPa	Poisons Ratio, -
Development	10.78±2.26	5.04±0.75	0.25±0.03
Ripening	7.18±1.29	5.12±0.86	0.21±0.07
Senescence	5.23±1.86	3.85±0.78	0.35±0.10

The value of skin elasticity modulus decreased with the stage of apple ripeness from 10.78 to 5.23 MPa. Modulus od elasticity for the flesh in development stage of ripeness was 5.04 MPa, for the ripening stage it slightly increased to 5.12 MPa, and then significantly decreased to a value of 3.85 MPa for the senescence stage of ripeness. The lowest Poisson's ratio value of 0.21, was achieved by the fruit at the ripening maturity stage. Fruit at the development maturity stage were slightly more prone to transverse deformations, with a Poisson's ratio of 0.25. The highest Poisson's ratio was observed for fruit at the senescence maturity stage, with a value of 0.35.

3.1. Strength Properties of Apple Fruit

Figure 5 and 6 present the averaged results of compression tests for three maturity stages. The original test data of force-displacement curves are shown in Figure 5a, while Figure 5b presents curves modified according to the methodology outlined in Figure 3 in chapter 2.4. Figure 6a shows the surface pressure as a function of force, while Figure 6b presents the contact surface as a function of force. The results presented in both figures are included in Table 4, divided into elastic region, plastic region and the region of a total flesh failure, for all stages of fruit ripeness (according to the methodology described on Figure 3).

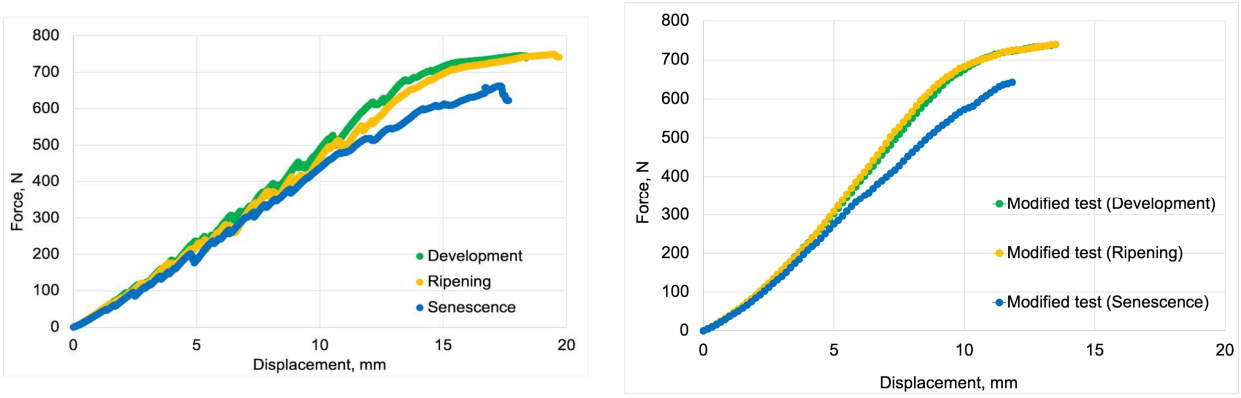

Figure 5. Averaged force-displacement curves of compression tests for three stages of fruit ripening: (**a**) original test curve, (**b**) modified test curve.

 doi:10.20944/preprints202409.0825.v2

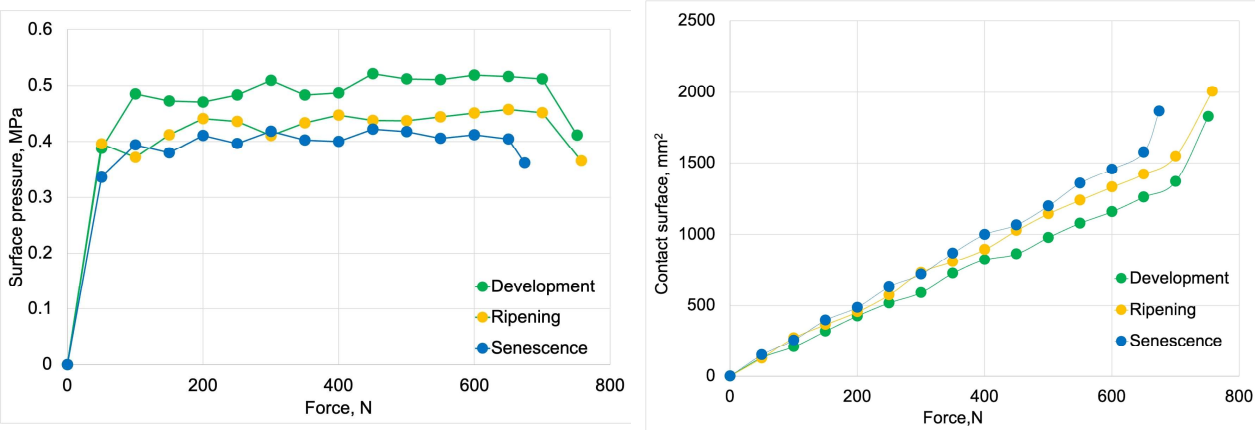

(a) (b)

Figure 6. Averaged surface mapping results obtained during compression testing for three stages of fruit ripening: (**a**) Surface pressure curves as a function of loading, (**b**) Contact surface as a function of loading.

Table 4. Results of mechanical testing of whole fruit obtained from force-displacement curves and surface pressure-force curves.

Region 1 - Elastic region				
Stage of ripeness	Inflection point, N	Displacement, mm	Contact Surface, mm²	Surface Pressure, MPa
Development	344.72±3.45	7.31±0.29	723.41±76.67	0.49±0.039
Ripening	339.14±5.96	7.55±0.28	806.24±25.99	0.44±0.014
Senescence	262.41±2.58	4.73±0.38	630.65±49.82	0.40±0.034
Region 2 - Plastic region				
Stage of ripeness	Flesh failure point, N	Displacement, mm	Contact Surface, mm²	Surface Pressure, MPa
Development	646.15±8.47	12.98±0.34	1258.8.4±79.98	0.52±0.031
Ripening	658.76±10.14	13.16±0.57	1419.60±116.64	0.46±0.037
Senescence	576.95±67.24	12.99±1.27	1355.80±213.119	0.41±0.065
Region 3 - Final failure				
Stage of ripeness	Skin failure point, N	Displacement, mm	Contact Surface, mm²	Surface Pressure, MPa
Development	751.29±8.47	19.02±0.76	1826.00±163.24	0.41±0.038
Ripening	757.50±10.14	20.42±1.17	2005.20±123.45	0.38±0.014
Senescence	674.18±67.24	17.95±2.41	1865.20±212.65	0.36±0.045

Comparing Figures 5a and 5b, it can be seen that after compensating for the local force drops, we see that fruit at the stage of ripening maturity were characterized by slightly greater strength in the plastic region. This also means that these drops in force were either more frequent or had greater values.

Based on Table 4, it can be observed that as apples progressed through the stages of development, plastic deformations began at lower force values. Similarly, the force causing the disruption of the flesh tissue structure also decreased with the ripening stage. However, when the flesh in the compression axis ceased to transmit loads due to the disruption of its cohesive connection

 doi:10.20944/preprints202409.0825.v2

with the seed nest, it was found that fruit at the ripening stage were the last to crack, at the highest force and displacement value.

From the surface pressure results presented in Figure 6 and Table 4, it is evident that as the fruit matures, the contact surface increases (Figure 6b), leading to a decrease in surface pressures. Throughout the entire compression process, it can also be observed that they remain at a consistent level within the range corresponding to their maturity stage (Figure 6a).

3.1. Bruises Volume

Figure 7 presents the results of apple bruise volumes determined based on tomographic images. The graph is divided into load ranges (20%, 50%, and 80% of Failure Force) and maturity stages. The study showed that regardless of the load range, the extent of bruising slightly increased during the transition from the development stage to the ripening stage achieving the highest values and then obtained the lowest value at the senescence stage.

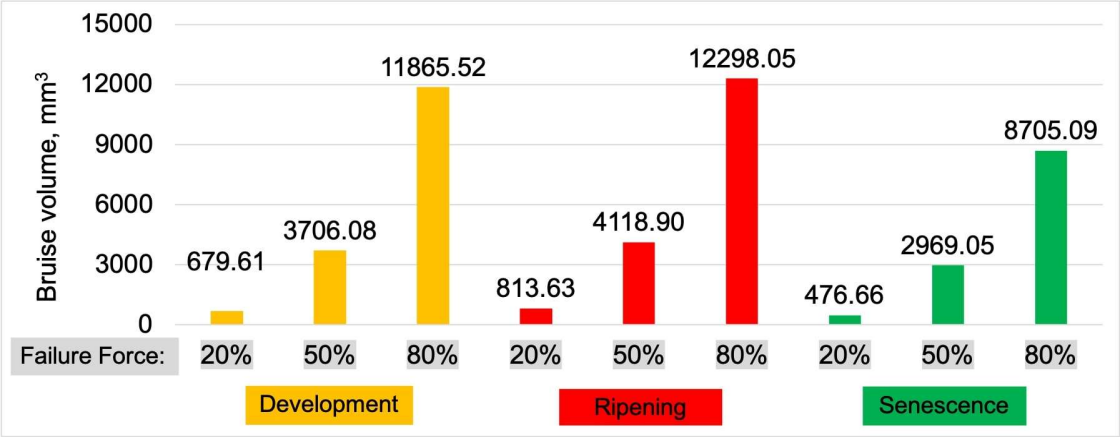

Figure 7. Results of fruit bruise volume, determined for three load ranges and three ripening stages.

These results, especially for the ripening maturity, have allowed us to formulate research hypothesis discussed in detail in the discussion section.

4. Discussion

The new variety of apples, Chopin, is highly regarded by researchers. The fruit has been studied in terms of i) the effect of storage conditions on the content of molecules [2] and storability and nutritional value [1], ii) bioactive compounds, antioxidant potential and cultivar functional properties [31,32], iii) The effect of mycorrhizal fungi and PGPR on tree nutritional status and growth [32], iv) quality and nutritional value in relation to popular apples growing in Poland [3]. This article explores different issues than those previously addressed by researchers, thereby providing a good complement to the current state of knowledge. Now the practical application of mechanical research on fruit is even more evident, especially since robotic fruit harvesting is becoming increasingly popular, and designing devices for this purpose requires defining the mechanical properties of the fruit [33,34].

The research presented in this article confirmed the need to carefully take into account the maturity stage in mechanical research, and in particular in the construction of MES models for the food industry. The results of mechanical and Micro-CT tests for specific and verified stages of apple ripeness provided a complete dataset for building and validating elastic and elastic-plastic FE models in different article [28]. Further conclusions on the superiority of elastoplastic models over viscoelastic ones (for tissue models covering the full range of fruit loading) require dedicated studies focused exclusively on the adaptation of various material types, such as elastic, elastoplastic, viscoelastic, crushable foam, and others.

 doi:10.20944/preprints202409.0825.v2

Fruit at the stage of ripening maturity was characterized by the highest elastic modulus of the flesh tissue, higher strength of whole fruit in plastic region (based on modified charts showing force-displacement curves), the highest value of the final apple destructive force, but not the highest strength in a significant part of the whole apple compression process, and not the highest resistance to bruising. Results of Micro-Ct and the results of modified and real compression tests of whole fruit have allowed us to formulate the research hypothesis regarding the influence of flesh cracking (characterized by local drops of force), influencing the bruise visibility and detection.

It's important to note that bruises visible in microtomographic images are apparent due to the leakage of cell sap and the tearing of flesh tissue to such an extent that the detection of discontinuity in the foam structure of the apple flesh is possible. Therefore, delving into the cellular structure and understanding the mechanism of apple fruit behavior is so crucial for a comprehensive description of the phenomena occurring in the tissue at different stages of loading, with particular emphasis on their ripening stages. According to [35] process of gas diffusion, rupture of intercellular connections, cracking of cell walls, and migration of cell sap throughout the tissue should be considered to fully define the behavior of the apple flesh under load. Creating a coherent and uniform theory of mechanics for biological materials would lead to a system of equilibrium equations with a complex structure with many variables. Such a system would have to include solutions in the field of biochemistry, biomechanics, and biophysics [36].

6. Conclusions

- The study demonstrated that the mechanical behavior of apples is strongly influenced by ripening stage, which must be precisely accounted for when constructing FEM models for food industry applications.
- A complete dataset of mechanical properties and Micro-CT-based bruise volumes was developed for three distinct maturity stages of Chopin apples, supporting both material model definition and validation.
- The findings indicate that flesh cracking during compression, visible as local force drops, may play a key role in bruise visibility and detection, forming the basis for a new research hypothesis.
- Among the maturity stages, apples in ripening maturity exhibited the highest destructive force and elastic modulus, though not the highest resistance to bruising, indicating complex structural dynamics.
- The mechanical characterization of the Chopin cultivar, previously studied mainly in terms of biochemical properties, provides novel insights relevant to the design of robotic harvesting systems and mechanical fruit handling.

Author Contributions: Conceptualization, M.S. and R.S.; methodology, M.S.; software, M.S.; validation, M.S.; formal analysis, M.S.; investigation, M.S.; resources, M.S.; data curation, M.S.; writing—original draft preparation, M.S. and A.F.; writing—review and editing, M.S and A.F..; visualization, M.S.; supervision, R.S.; project administration, M.S.; funding acquisition, M.S. and A.F. All authors have read and agreed to the published version of the manuscript."

Funding: This work was supported by the Polish National Science Centre [2021/41/N/NZ9/02874]

Data Availability Statement: Data will be made available on request.

Acknowledgments: In this section, you can acknowledge any support given which is not covered by the author contribution or funding sections. This may include administrative and technical support, or donations in kind (e.g., materials used for experiments).

Conflicts of Interest: The authors declare no conflicts of interest.

 doi:10.20944/preprints202409.0825.v2

References

1. Kistechok, A.; Wrona, D.; Krupa, T. Effect of Storage Conditions on the Storability and Nutritional Value of New Polish Apples Grown in Central Poland. *Agriculture (Switzerland)* **2024**, *14*. https://doi.org/10.3390/agriculture14010059.
2. Ponder, A.; Jariené, E.; Hallmann, E. The Effect of Storage Conditions on the Content of Molecules in Malus Domestica 'Chopin' Cv. and Their In Vitro Antioxidant Activity. *Molecules* **2022**, *27*. https://doi.org/10.3390/molecules27206979.
3. Kistechok, A.; Wrona, D.; Krupa, T. Quality and Nutritional Value of 'Chopin' and Clone 'JB' in Relation to Popular Apples Growing in Poland. *Agriculture (Switzerland)* **2022**, *12*. https://doi.org/10.3390/agriculture12111876.
4. Noiton, D.A.M.; Alspach, P.A. *Founding Clones, Inbreeding, Coancestry, and Status Number of Modern Apple Cultivars*; 1996; Vol. 121;.
5. Zygmunt Hejnowicz *Anatomia i Histogeneza Roślin Naczyniowych*; Wydawnictwo Naukowe PWN: Warszawa, 2002; Vol. 1;.
6. Pratt, C. *Apple Flower and Fruit: Morphology and Anatomy*; 1988;
7. Zdunek, A.; Kozioł, A.; Cybulska, J.; Lekka, M.; Pieczywek, P.M. The Stiffening of the Cell Walls Observed during Physiological Softening of Pears. *Planta* **2016**, *243*, 519–529. https://doi.org/10.1007/s00425-015-2423-0.
8. Billy, L.; Mehinagic, E.; Royer, G.; Renard, C.M.G.C.; Arvisenet, G.; Prost, C.; Jourjon, F. Relationship between Texture and Pectin Composition of Two Apple Cultivars during Storage. *Postharvest Biol Technol* **2008**. https://doi.org/10.1016/j.postharvbio.2007.07.011.
9. Videcoq, P.; Barbacci, A.; Assor, C.; Magnenet, V.; Arnould, O.; Le Gall, S.; Lahaye, M. Examining the Contribution of Cell Wall Polysaccharides to the Mechanical Properties of Apple Parenchyma Tissue Using Exogenous Enzymes. *J Exp Bot* **2017**, *68*, 5137–5146. https://doi.org/10.1093/jxb/erx329.
10. Bich, L.; Pradeu, T.; Moreau, J.F. Understanding Multicellularity: The Functional Organization of the Intercellular Space. *Front Physiol* **2019**, *10*. https://doi.org/10.3389/fphys.2019.01170.
11. Wei, J.; Ma, F.; Shi, S.; Qi, X.; Zhu, X.; Yuan, J. Changes and Postharvest Regulation of Activity and Gene Expression of Enzymes Related to Cell Wall Degradation in Ripening Apple Fruit. *Postharvest Biol Technol* **2010**, *56*, 147–154. https://doi.org/10.1016/j.postharvbio.2009.12.003.
12. Contigiani, E. V.; Jaramillo-Sánchez, G.; Castro, M.A.; Gómez, P.L.; Alzamora, S.M. Postharvest Quality of Strawberry Fruit (Fragaria x Ananassa Duch Cv. Albion) as Affected by Ozone Washing: Fungal Spoilage, Mechanical Properties, and Structure. *Food Bioproc Tech* **2018**, *11*, 1639–1650. https://doi.org/10.1007/s11947-018-2127-0.
13. Juxia, W.; Qingliang, C.; Hongbo, L.; Yaping, L. Experimental Research on Mechanical Properties of Apple Peels. *Journal of Engineering and Technological Sciences* **2015**, *47*, 688–705. https://doi.org/10.5614/j.eng.technol.sci.2015.47.6.8.
14. Li, Z.; Thomas, C. Quantitative Evaluation of Mechanical Damage to Fresh Fruits. *Trends Food Sci Technol* **2014**, *35*, 138–150. https://doi.org/10.1016/j.tifs.2013.12.001.
15. Farkas, Cs.; Petróczki, K.; Fenyvesi, L. Method for Measuring Fruit Failure Caused by Different Mechanical Loads. *Hungarian Agricultural Engineering* **2016**, 51–54. https://doi.org/10.17676/hae.2016.29.51.
16. Mayorga-Martínez, A.A.; Olvera-Trejo, D.; Elías-Zúñiga, A.; Parra-Saldívar, R.; Chuck-Hernández, C. Non-Destructive Assessment of Guava (Psidium Guajava L.) Maturity and Firmness Based on Mechanical Vibration Response. *Food Bioproc Tech* **2016**, *9*, 1471–1480. https://doi.org/10.1007/s11947-016-1736-8.

 doi:10.20944/preprints202409.0825.v2

17. Fathizadeh, Z.; Aboonajmi, M.; Beygi, S.R.H. Nondestructive Firmness Prediction of Apple Fruit Using Acoustic Vibration Response. *Sci Hortic* **2020**, *262*. https://doi.org/10.1016/j.scienta.2019.109073.
18. Fadiji, T.; Coetzee, C.; Pathare, P.; Opara, U.L. Susceptibility to Impact Damage of Apples inside Ventilated Corrugated Paperboard Packages: Effects of Package Design. *Postharvest Biol Technol* **2016**, *111*, 286–296. https://doi.org/10.1016/j.postharvbio.2015.09.023.
19. Stropek, Z.; Gołacki, K. A New Method for Measuring Impact Related Bruises in Fruits. *Postharvest Biol Technol* **2015**, *110*, 131–139. https://doi.org/10.1016/j.postharvbio.2015.07.005.
20. Diels, E.; van Dael, M.; Keresztes, J.; Vanmaercke, S.; Verboven, P.; Nicolai, B.; Saeys, W.; Ramon, H.; Smeets, B. Assessment of Bruise Volumes in Apples Using X-Ray Computed Tomography. *Postharvest Biol Technol* **2017**, *128*, 24–32. https://doi.org/10.1016/j.postharvbio.2017.01.013.
21. Van De Looverbosch, T.; Vandenbussche, B.; Verboven, P.; Nicolaï, B. Nondestructive High-Throughput Sugar Beet Fruit Analysis Using X-Ray CT and Deep Learning. *Comput Electron Agric* **2022**, *200*. https://doi.org/10.1016/j.compag.2022.107228.
22. Herremans, E.; Melado-Herreros, A.; Defraeye, T.; Verlinden, B.; Hertog, M.; Verboven, P.; Val, J.; Fernández-Valle, M.E.; Bongaers, E.; Estrade, P.; et al. Comparison of X-Ray CT and MRI of Watercore Disorder of Different Apple Cultivars. *Postharvest Biol Technol* **2014**, *87*, 42–50. https://doi.org/10.1016/j.postharvbio.2013.08.008.
23. Wang, L.J.; Zhang, Q.; Song, H.; Wang, Z.W. Mechanical Damage of 'Huangguan' Pear Using Different Packaging under Random Vibration. *Postharvest Biol Technol* **2022**, *187*. https://doi.org/10.1016/j.postharvbio.2022.111847.
24. Bejaei, M.; Stanich, K.; Cliff, M.A. Modelling and Classification of Apple Textural Attributes Using Sensory, Instrumental and Compositional Analyses. *Foods* **2021**, *10*. https://doi.org/10.3390/foods10020384.
25. Stopa, R.; Szyjewicz, D.; Komarnicki, P.; Kuta, Ł. Determining the Resistance to Mechanical Damage of Apples under Impact Loads. *Postharvest Biol Technol* **2018**, *146*, 79–89. https://doi.org/10.1016/j.postharvbio.2018.08.016.
26. Tomala, K.; Grzęda, M.; Guzek, D.; Głąbska, D.; Gutkowska, K. The Effects of Preharvest 1-Methylcyclopropene (1-MCP) Treatment on the Fruit Quality Parameters of Cold-Stored 'Szampion' Cultivar Apples. *Agriculture (Switzerland)* **2020**, *10*. https://doi.org/10.3390/agriculture10030080.
27. Pijanowski E.; Mrożewski S.; Horubała A.; Jarczyk A. *Technologia Produktów Owocowych i Warzywnych*; PWRiL: Warszawa, 1973;
28. Słupska, M.; Stopa, R.; Figiel, A. 3D FEM Modeling of Polish Apple 'Chopin': Elastic vs. Elastoplastic Behavior Across Maturity Stages. *Preprints (Basel)* **2024**. https://doi.org/10.20944/preprints202409.0987.v1.
29. Komarnicki, P.; Stopa, R.; Szyjewicz, D.; Młotek, M. Evaluation of Bruise Resistance of Pears to Impact Load. *Postharvest Biol Technol* **2016**, *114*, 36–44. https://doi.org/10.1016/j.postharvbio.2015.11.017.
30. Komarnicki, P.; Stopa, R.; Szyjewicz, D.; Kuta, Ł.; Klimza, T. Influence of Contact Surface Type on the Mechanical Damages of Apples Under Impact Loads. *Food Bioproc Tech* **2017**, *10*, 1479–1494. https://doi.org/10.1007/s11947-017-1918-z.
31. Sawicka, M.; Latocha, P.; Łata, B. Peel to Flesh Bioactive Compounds Ratio Affect Apple Antioxidant Potential and Cultivar Functional Properties. *Agriculture (Switzerland)* **2023**, *13*. https://doi.org/10.3390/agriculture13020478.
32. Przybyłko, S.; Kowalczyk, W.; Wrona, D. Article the Effect of Mycorrhizal Fungi and Pgpr on Tree Nutritional Status and Growth in Organic Apple Production. *Agronomy* **2021**, *11*. https://doi.org/10.3390/agronomy11071402.

 doi:10.20944/preprints202409.0825.v2

33. Ji, W.; Qian, Z.; Xu, B.; Tang, W.; Li, J.; Zhao, D. Grasping Damage Analysis of Apple by End-Effector in Harvesting Robot. *J Food Process Eng* **2017**, *40*. https://doi.org/10.1111/jfpe.12589.
34. Jia, W.; Zhang, Y.; Lian, J.; Zheng, Y.; Zhao, D.; Li, C. Apple Harvesting Robot under Information Technology: A Review. *Int J Adv Robot Syst* 2020, *17*.
35. Roman Stopa Modelowanie Deformacji Korzenia Marchwi w Warunkach Obciążeń Skupionych Metodą Elementów Skończonych. Monografia, Wydawnictwo Uniwersytetu Przyrodniczego we Wrocławiu: Wrocław, 2010.
36. Murase, H.; Merva, G.E.; Segerlind, L.J.; Member Member Member, A.; Asae, A.; Abstract, A. *Variation of Young's Modulus of Potato as A Function of Water Potential*; 1980;